

Energy Spectra and Angular Distributions of Photoneutrons from Heavy Nuclei*†

GLENN A. PRICE‡

Physics Research Laboratory, University of Illinois, Champaign, Illinois

(Received November 9, 1953)

The energy spectra of photoneutrons from the absorption of 22-Mev bremsstrahlung by silver and bismuth have been measured with nuclear emulsions. Comparisons are made between the observed photoneutron spectra and those predicted on the basis of a statistical nuclear model. Energy level densities are assumed proportional to $\exp[(a\epsilon)^2]$ and $\ln(A\epsilon/20+1)$, where ϵ is the excitation energy of the residual nucleus. The exponential form of the energy level density is in better agreement with the data than is the logarithmic form. However, for neutron energies greater than 4 Mev there are more photoneutrons observed than predicted by the exponential energy level density scheme.

The angular distributions of photoneutrons from several elements have been measured with a variety of neutron detectors. The moderated neutron detector, which is equally sensitive to neutrons of most energies, indicates the photoneutron flux to be predominately isotropic. The small anisotropic component has a maximum at 90 degrees to the x-ray beam. Photoneutrons from bismuth have a larger anisotropic component than photoneutrons

from any other element which was tested. In that case 21 percent of the neutron flux is in the anisotropic component.

The $\text{Al}(n,p)$ and $\text{Si}(n,p)$ reactions have been used to measure the angular distributions of photoneutrons from several elements. These reactions have thresholds at 1.95 Mev and 2.69 Mev, respectively and are primarily sensitive to neutrons with more than 4-Mev energy. The angular distributions thus observed have a maximum at 90 degrees to the x-ray beam. In general, photoneutrons from the heavy elements deviate more from isotropy than do the light elements. An epithermal neutron detector indicates that the low-energy photoneutrons are emitted isotropically.

It is concluded that most photoneutrons are generated in a manner consistent with the statistical nuclear model. The high-energy photoneutrons, which constitute a small fraction of the total photoneutron flux, are ejected predominately at right angles to the x-ray beam as expected by dipole absorption of the photons.

I. INTRODUCTION

PREVIOUS measurements of the angular distribution of photoneutrons by Price and Kerst¹ indicated that photoneutrons from heavy nuclei are predominately isotropic in space. Byerly² has measured the photoneutron energy spectra from copper and found the measurement to be in agreement with a statistical nuclear model. However, detailed examination of the angular distributions of photoneutrons from heavy nuclei by Poss³ and by Demos, Fox, Halpern, and Koch⁴ has shown that the high-energy photoneutrons are emitted anisotropically in space with a maximum at right angles to the x-ray beam. Experiments by other investigators have revealed similar characteristics in gamma-proton reactions.⁵⁻¹⁰ The experiments described in this paper were performed to gain more information concerning gamma-neutron reactions in heavy nuclei using 22-Mev bremsstrahlung from a betatron.

II. PHOTONEUTRON ENERGY SPECTRA

The presence of knock-on protons in nuclear emulsions was used to measure the energy and number of

photoneutrons which were ejected at right angles to the 22-Mev x-ray beam incident on silver and bismuth targets. The Ilford C-2, 200-micron emulsions were wrapped in black paper and placed with their leading edges 6 in. from the target. A lead shield, $\frac{1}{32}$ in. thick, was placed between the target and the emulsion to absorb a soft ionizing radiation which otherwise would have excessively fogged the plates. The lead shield was sufficiently transparent to neutrons so that no correction was required in computing the neutron flux. The emulsion was tilted 3 degrees from the target so that the leading edge of the emulsion would not shield the rest of the emulsion. The emulsions were shielded from x-rays and neutrons originating at the betatron by thick walls of concrete and paraffin.

The silver target was a sphere, 1.75 cm in diameter and weighed 27.9 grams. After correcting for x-ray absorption in the target the integrated exposure for the silver target was 134.2 mole-"r." The bismuth target was 1.615 cm in diameter and weighed 21.5 grams. After correcting for x-ray absorption in the target the integrated exposure for the bismuth target was 45.2 mole-"r." In both cases the correction for x-ray absorption in the targets amounted to about 36 percent. Exposure times for all runs were 105 minutes. The total number of "r" in each run was monitored by comparing the intensity of 8.2-hour beta activity induced in a tantalum foil at the exit port of the lead collimator with the tantalum activity when a Victoreen ion chamber (in an aluminum block) was placed in the x-ray beam.

After the emulsions were developed by appropriate procedures they were scanned with an E. Leitz Wetzlar binocular microscope, 12X ocular and 8-mm objective. All proton tracks which started and stopped in the

* Assisted by the joint program of the U. S. Office of Naval Research and the U. S. Atomic Energy Commission.

† Part of a thesis submitted in partial fulfillment of the requirement for the degree of Doctor of Philosophy in Physics in the Graduate College of the University of Illinois.

‡ Now at Brookhaven National Laboratory, Upton, New York.

¹ G. A. Price and S. W. Kerst, *Phys. Rev.* **77**, 806 (1950).

² P. R. Byerly, Jr., thesis, University of Pennsylvania, 1950 (unpublished).

³ H. L. Poss, *Phys. Rev.* **79**, 539 (1950).

⁴ Demos, Fox, Halpern, and Koch, *Phys. Rev.* **86**, 605 (1952).

⁵ B. C. Diven and G. M. Almy, *Phys. Rev.* **80**, 407 (1950).

⁶ Curtis, Hornbostel, Lee, and Salant, *Phys. Rev.* **77**, 290 (1950).

⁷ J. Halpern and A. K. Mann, *Phys. Rev.* **83**, 370 (1951).

⁸ Rothman, Mann, and Halpern, *Phys. Rev.* **86**, 629 (1952).

⁹ M. E. Toms and W. E. Stephens, *Phys. Rev.* **82**, 709 (1951).

¹⁰ M. E. Toms and W. E. Stephens, *Phys. Rev.* **85**, 728 (1952).

emulsion, and whose directions were within 15 degrees of the neutron direction were accepted. The neutron energy was determined from the range and direction of the knock-on proton in the emulsion. The number of neutrons in any energy interval in calculated from the number of proton tracks observed in that energy interval, the hydrogen content of the emulsion, and the neutron-proton scattering cross section. Appropriate corrections were made for the probability of protons leaving the emulsion before the ends of the range, probability that the proton angle is less than 15 degrees, and the scattering of neutrons by heavy nuclei in the nuclear emulsion.

The photoneutron energy spectra are shown in Figs. 1 and 2. In the case of the bismuth photoneutron spectrum, Fig. 1, the neutrons were computed in 1-Mev intervals. However, for the silver photoneutrons spectrum, Fig. 2, the neutrons were put into 2-Mev intervals because of the larger probable errors involved. The probable errors as indicated by vertical lines through the experimental points represent variations in neutron intensity if the number of proton tracks, N , which contribute to each point is varied by $\pm\sqrt{N}$.

The photoneutron energy spectrum with the silver target was taken from 129 acceptable proton tracks found in 462 mm² of emulsion. The bismuth photoneutron spectrum was calculated from 196 proton tracks in 467 mm² of emulsion. The background plates yielded 61 tracks for a corresponding area. 58 of the 61 background tracks were in the energy range from 1 to 2 Mev. The background plates were exposed in a manner similar to the regular plates but with no target in the x-ray beam. Unexposed nuclear emulsions

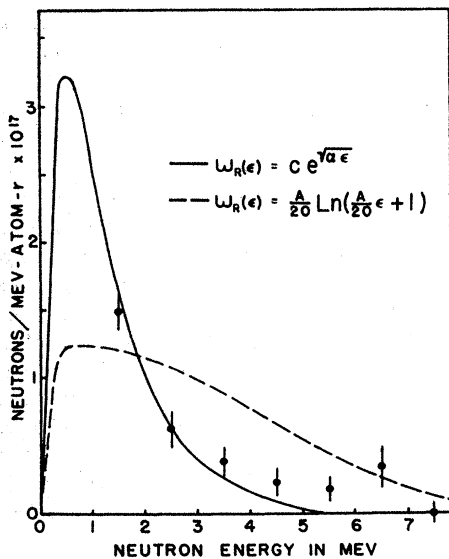


FIG. 1. Energy spectrum of photoneutrons emitted from bismuth when irradiated by 22-Mev bremsstrahlung. Solid and dashed curves indicated predicted spectra as calculated on the statistical model of the nucleus with indicated energy level densities, $\omega_R(\epsilon)$.

revealed a large number of one, three, four, and five prong alpha stars which were attributed to thorium contamination. The one-prong alpha tracks could not be easily distinguished from short proton tracks. Consequently, most of the 58 background tracks from 1 to 2 Mev could be attributed to single-prong alpha stars. If fresh nuclear emulsions had been used the effect of thorium contamination would have been much less.

The solid and dashed curves in Figs. 1 and 2 represent photoneutron spectra which would be expected on the basis of a statistical nuclear model. The number of neutrons/Mev-atom-cm, $F(\epsilon_n)$, was calculated from the following formula, which is analogous to one derived by Diven and Almy for photoproton spectra,

$$F(\epsilon_n) = \epsilon_n \sigma_{n\beta} \int_{B_n + \epsilon_n}^{E_{\max}} \frac{\sigma(\gamma, n) N(E, E_{\max}) \omega_R(E - B_n - \epsilon_n)}{\int_0^{E - B_n} \epsilon_n \sigma_{n\beta} \omega_R(E - B_n - \epsilon) d\epsilon_n} dE,$$

where ϵ_n is the neutron energy, $\sigma_{n\beta}$ is the neutron penetration factor, E is the photon energy, B_n is the neutron binding energy, $\sigma(\gamma, n)$ is the gamma-neutron cross section, $N(E, E_n)$ is the number of photons/Mev-cm² in the bremsstrahlung spectrum, and $\omega_R(E - B_n - \epsilon_n)$ is the energy level density of the residual nucleus. The quantity, $E - B_n - \epsilon_n$, is the excitation energy of the residual nucleus.

The solid curves are the theoretical photoneutron energy spectra which would be expected with an energy level density,

$$\omega_R(E - B_n - \epsilon_n) = C \exp\{[a(E - B_n - \epsilon_n)]^{\frac{1}{2}}\},$$

where C is a constant, $a = 1.6(A - 40)^{\frac{1}{2}}$, and A is the atomic mass number.

The dashed curves are the theoretical photoneutron energy spectra which would be expected with an energy level density,

$$\omega_R(E - B_n - \epsilon_n) = (A/20) \ln[(A/20)(E - B_n - \epsilon_n) + 1].$$

The exponential form of the energy-level density is suggested by Weisskopf and Ewing,¹¹ whereas the logarithmic form is the Schiff¹² regular energy-level density.

$\sigma(\gamma, n)$ for silver was taken from the results of Diven and Almy. The gamma-neutron cross section for bismuth has not been measured; therefore an assumed cross section was used. The bismuth gamma-neutron cross section was assumed to have a threshold at 7.5 Mev, a peak at 13.5 Mev, a full width at half-maximum of 6 Mev, and an integrated cross section of 7.5 Mev-barns. The bismuth threshold has been measured by Sher, Halpern, and Mann,¹³ and the integrated cross section is inferred from the total photoneutron yields

¹¹ V. F. Weisskopf and D. H. Ewing, Phys. Rev. **57**, 472 (1940).

¹² L. I. Schiff, Phys. Rev. **73**, 1311 (1948).

¹³ Sher, Halpern, and Mann, Phys. Rev. **84**, 149 (1951).

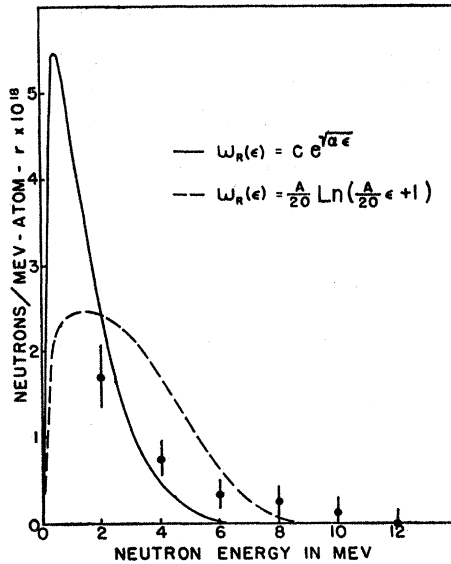


FIG. 2. Energy spectrum of photoneutrons emitted from silver when irradiated by 22-Mev bremsstrahlung. Solid and dashed curves indicate predicted spectra as calculated on the statistical model of the nucleus with indicated energy level densities, $\omega_R(\epsilon)$.

by Kerst and Price.¹⁴ The photoneutron energy spectrum is quite insensitive to the shape of the gamma-neutron cross section to the assumption concerning the shape of the cross section is not a crucial one. The neutron penetration factor $\sigma_{n\beta}$ was calculated from a formula given by Weisskopf.¹⁵

III. ANGULAR DISTRIBUTIONS OF PHOTONEUTRONS

A. Moderated Neutron Detector

The moderated neutron detector is the same one which was used by Price and Kerst to measure the angular distribution of photoneutrons. It is patterned after the shielded long counter of Hanson and McKibben¹⁶ except that it uses a rhodium foil instead of a BF_3 counter for detecting slow neutrons. It consists of a cylindrical rhodium foil in a hole in a block of paraffin, $2\frac{3}{4}$ in. \times $2\frac{3}{4}$ in. \times $5\frac{1}{4}$ in. The paraffin block is surrounded by $\frac{1}{2}$ in. cadmium foil and is placed in a paraffin cylinder, 12 in. in diameter and 15 in. long. The action of the detector is as follows: photoneutrons having more energy than 0.1 ev pass through the cadmium, are slowed down by collisions with hydrogen nuclei in the smaller paraffin block and are captured by the rhodium foil. Neutrons which come in toward the side or back of the detector are slowed down in the paraffin cylinder and then are captured in the cadmium foil. Thus, the action of the paraffin cylinder and cadmium foil make the detector sensitive to neutrons

¹⁴ D. W. Kerst and G. A. Price, Phys. Rev. **79**, 725 (1950).

¹⁵ McMillan, Segrè, Teller, Bloch, Williams, Critchfield, Weisskopf, and Christy, U. S. Atomic Energy Commission Report, MDDC-1175, 1947 (unpublished).

¹⁶ W. Sleator, Jr., Phys. Rev. **72**, 207 (1947).

from one direction only. The energy spectrum of photoneutrons is such that eliminating neutrons less than 0.1 ev in energy has a negligible effect on the results. When a normal Rh^{103} nucleus captures a slow neutron it forms Rh^{104} which decays by beta emission with a 44-second half-life. Consequently, a measure of the 44-second beta activity gives a relative yield figure for the photoneutron intensity from the target.

A large concrete wall shields the neutron detector from x-rays and neutrons which originate at the betatron. Another rhodium foil was placed in a crevice in the concrete wall for the purpose of measuring the relative intensity of the x-ray beam. The hydrogen in the concrete wall has a moderating action on the neutrons which are generated at the electron target in the betatron, the x-ray collimator, and in the concrete wall by x-rays. Consequently, the slow neutron flux in the concrete wall is proportional to the intensity of the x-ray beam passing through the collimator, provided that the direction of the beam does not shift. Thus, the intensity of 44-second beta activity in the monitor foil is proportional to the integrated x-ray intensity at the target. This type of x-ray monitor has the particular advantage that it has the same rate of decay as the neutron detector. Therefore, fluctuations in photoneutron yield due to fluctuations in x-ray intensity during a run are nullified.

The procedure in making a run was to expose a sample to three minutes radiation by the betatron with rhodium foils in place. Then 30 seconds were allowed to move the rhodium foils to two thin-walled cylindrical Geiger counters. The total counts on the two Geiger counters for the next three minutes give the relative

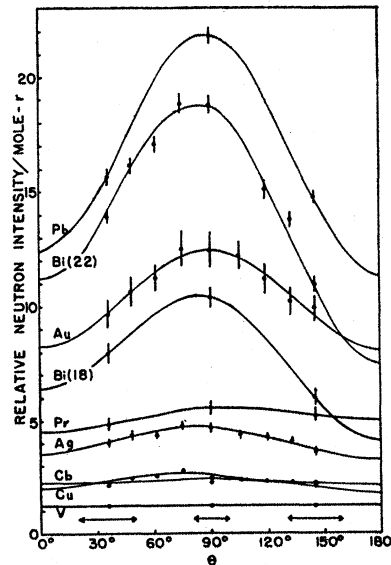


FIG. 3. Angular distributions of high-energy photoneutrons created by 22-Mev bremsstrahlung on various targets as observed with the $\text{Al}^{27}(n,p)$ detector. The bismuth target was also irradiated with 18-Mev bremsstrahlung.

measure of the neutron yield and the x-ray intensity, respectively. Then a background run was made by repeating the previous procedure with no target in the x-ray beam. The cycle for one run was completed in 10 minutes, which allowed plenty of time for the decay of activity in the foils between runs.

The angular distributions of total neutron intensity as observed with the moderated neutron detector are shown in figure.³ Each point in Fig. 3 represents the average of three runs with the exception of silver and gold. The silver and gold values are averages of two complete series which were taken on separate days, or an average of six runs each. The agreement between the repeated values was well within the probable errors as calculated from the statistics of counting rates. Target sizes varied from 0.15-gram mole for the gold and bismuth targets to 9.1-gram mole for the beryllium target, although most of the targets contained less than one gram mole.

An estimate of the fraction of neutrons scattered by the bismuth target into the moderated neutron detector was made. This was done because the neutron detector cannot distinguish photoneutrons which originate at the target from other neutrons, say, which originate at the betatron and are scattered by the target into the detector. The moderated neutron detector was used without its cadmium shield and outer paraffin cylinder to measure the neutron flux in the x-ray beam at the target position. If the mean scattering cross section of bismuth is taken to be 8 barns, then the fraction of scattered neutrons observed at the 90-degree position would be 1.3 percent of the photoneutron yield observed at that position. In the case of gold the strong resonance at 4.8 ev might scatter enough neutrons to account for the observed asymmetric distribution of neutrons.

The smooth curves through the experimental points of Fig. 3 are the best fit of the data to the function, $a_0 + a_1 P_1(\cos\theta) + a_2 P_2(\cos\theta)$ where a_0 , a_1 , and a_2 are arbitrary constants and $P_1(\cos\theta)$ and $P_2(\cos\theta)$ are Legendre polynomials.

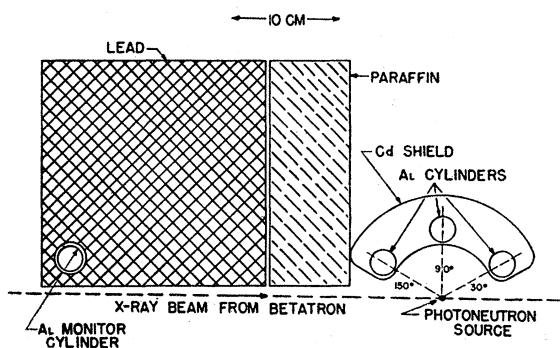


FIG. 4. Experimental setup for observation of angular distributions of photoneutrons with threshold detectors.

B. $\text{Al}^{27}(n,p)$ Neutron Detector

A series of aluminum cylinders was used to observe the angular distributions of fast photoneutrons using 22-Mev bremsstrahlung. This method of detection makes use of the neutron-proton reaction in Al^{27} which leads to Mg^{27} which is beta-active with a 10.2-minute half-life. The threshold for the $\text{Al}^{27}(n,p)$ reaction is 1.95 Mev, and the relative cross section has been measured by Bretscher and Wilkinson¹⁷ for neutron energies up to 4 Mev. The $\text{Al}^{27}(n,p)$ neutron detector is primarily sensitive to neutrons with more than 4-Mev energy and is sensitive to a lesser degree to neutrons of lower energy.

The experimental setup for the use of $\text{Al}^{27}(n,p)$ detectors is shown in Fig. 4. The aluminum cylinders are made of pure aluminum, weigh 11.1 grams, are 3 in. long, and have an inside diameter of 13/16 in. The lead and paraffin blocks shield the aluminum cylinders from x-rays and neutrons which originate at the betatron. The cadmium box around the aluminum cylinders is necessary to absorb slow neutrons coming from the lead, the paraffin, and the room in general. Aluminum cylinders are positioned in the cadmium box by annular slots in a lucite sheet. Slow neutron capture in aluminum produces Al^{28} which is beta active with a 2.4-minute half-life. The 2.4-minute activity would confuse the analysis of the 10.2-minute activity if it were not eliminated. Tests with a Ra-Be neutron source, in which a paraffin reflector was used to increase the number of thermal neutrons, indicated that a $\frac{1}{16}$ -in. cadmium shield would completely eliminate the 2.4-min activity induced in the aluminum by slow neutrons without affecting the 10.2-minute activity.

The standard operating procedure included the use of three aluminum cylinders simultaneously at three different angles. All targets were cylinders less than $\frac{5}{8}$ in. in diameter and less than 2 in. high and oriented with the x-ray beam perpendicular to the axis of the cylinder. All targets were in the pure metallic form except for the praeosodymium target in which case PrO_2 was used. Target weights varied from 30.6 grams for the PrO_2 to 92.9 grams for the Cu target. The betatron was on for 15 minutes, followed by a 5-minute waiting period, during which time the aluminum cylinders were transferred to cylindrical Geiger counters, and then the total count for the next 15 minutes was taken as relative intensity of fast neutrons. There were nine aluminum cylinders, and they were alternated so that the 10.2-minute activity had sufficient time to decay between successive uses. The neutron flux at a particular angular position was taken from the average activity of the nine aluminum cylinders at that position. All runs were normalized to a constant x-ray intensity by means of an aluminum cylinder in a cadmium lined cavity in the lead block. Fast neutrons from the betatron

¹⁷ E. Bretscher and D. H. Wilkinson, Proc. Cambridge Phil. Soc. 45, 141 (1949).

and those generated in the lead block by x-rays give rise to a 10.2-minute beta activity in the monitor aluminum cylinder which is proportional to the integrated x-ray intensity at the target position.

The angular distributions of photoneutrons as observed with $\text{Al}^{27}(n,p)$ detectors are shown in Fig. 5. Vertical lines through each point indicate the standard deviation as determined from the counting statics. The smooth curves represent the least squares fit of the data to the function $a_0 + a_1 P_1(\cos\theta) + a_2 P_2(\cos\theta)$. Figure 6 gives the values of B/A if the fast photoneutron yield is fitted to the function $A + B^2 \sin^2\theta$. The betatron was operated with a maximum photon energy of 22 Mev in all cases except one run with a bismuth target in which case the betatron energy was 18 Mev. The relative neutron intensities are plotted in arbitrary units per

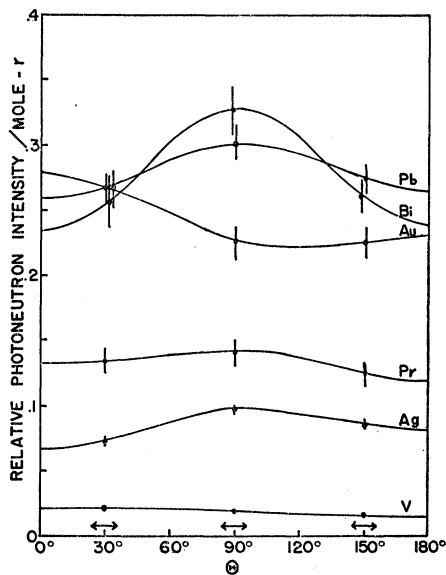


FIG. 5. Angular distributions of photoneutrons created by 22-Mev bremsstrahlung as observed with the moderated neutron detector. θ is the angle at the target between the incident bremsstrahlung and the neutron detector.

mole- τ ." On the same scale of arbitrary units a 500-mg RaBe source gives 3.29×10^{-6} arbitrary units per Ra-Be neutron. However, it is not possible to compare absolute numbers of fast photoneutrons with fast Ra-Be neutrons since the energy distributions of the two sources are not the same. The geometrical centers of the aluminum cylinders nearest the x-ray beam were at angles of 30 degrees and 150 degrees from the beam taken at the target. However, the mean angles of the detectors for the detection of neutrons were actually 36 degrees and 144 degrees. The mean angle of each detector was calculated with a $\sin^2\theta$ weighting factor since there was a large $\sin^2\theta$ component in the photoneutron intensities. The mean angle for detection differs from the geometrical center of the

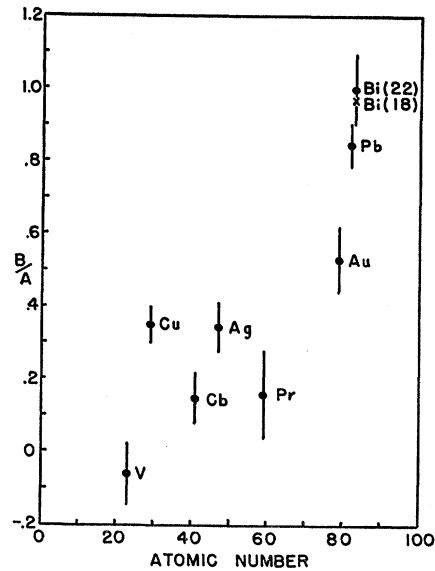


FIG. 6. Anisotropy of photoneutrons as observed with the $\text{Al}^{27}(n,p)$ threshold detector when the angular distributions are fitted to the function $A + B \sin^2\theta$.

cylinder because of the relatively large size in comparison to the distance from the photoneutron source.

The fast neutron detector was checked by means of a 500-mg Ra-Be neutron source. The Ra-Be source, which emits 6.17×10^6 neutrons per second, was put at the normal target position. Runs were made with the same time sequence as for a photoneutron run. Fast neutrons from Ra-Be were observed at nine angles from 30 degrees to 150 degrees. The probable error due to counting statistics was ± 0.75 percent and a maximum variation of 5 percent from the mean was observed from one position to another. Consequently the variations are real and can be attributed to errors in the positions of the annular slots of about $\frac{1}{32}$ in. Therefore, all observed neutron intensities were corrected for the variations observed with the Ra-Be neutrons, which should be emitted isotropically.

C. $\text{Si}^{28}(n,p)$ Neutron Detector

Another threshold detector for the observation of fast neutrons is the $\text{Si}^{28}(n,p)$ reaction. Al^{28} is unstable to the emission of a β particle with a half-life of 2.4 minutes. The threshold of the (n,p) reaction is 2.69 Mev and is probably most sensitive to neutrons of more than 5.5-Mev energy. The detectors were actually in the form of quartz cylinders, SiO_2 , about $1\frac{3}{4}$ in. long, $\frac{3}{4}$ -in. inside diameter, and $\frac{1}{32}$ -in. wall thickness. The method of using these SiO_2 detectors was similar to the method employed for $\text{Al}^{27}(n,p)$ detectors except that no cadmium box was used to stop slow neutrons since they do not create a competing activity. The intensity of the 2.4-minute beta activity in the quartz cylinders gives a relative value for the intensity of fast neutrons from the irradiated sample.

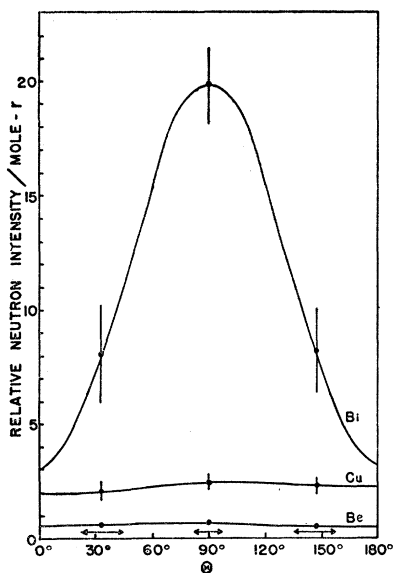


Fig. 7. Angular distributions of photoneutrons from 22-Mev bremsstrahlung on several targets as observed with the $\text{Si}^{28}(n,p)$ threshold detector.

The angular distributions of fast photoneutrons as observed with $\text{Si}^{28}(n,p)$ detectors are shown in Fig. 7. The smooth curves are the best fit of the data to the function, $a_0 + a_1P_1(\cos\theta) + a_2P_2(\cos\theta)$. The units of relative neutron intensity as observed with different types of neutron detectors in this paper bear no relationship to each other.

D. Epithermal Neutron Detector

A neutron detector was constructed which consisted of a rhodium foil in a paraffin cylinder 4.5 cm in diameter and 6 cm long. Moderately slow neutrons are slowed down in the paraffin to an energy at which they are readily captured by the rhodium. A measurement of the 44-second beta activity in the rhodium gives a relative yield value for the neutron flux. The paraffin block is small enough so that neutrons of more than a few hundred kev energy do not suffer collisions in passing through the paraffin and therefore are not detected.

In such a neutron detector the sensitivity should be fairly uniform for neutron energies from zero up to some value ϵ_0 , and above that value decrease rather rapidly. A measurement was made in which a small sample of heavy water was irradiated with 7-Mev bremsstrahlung, and the angular distribution of photoneutrons from deuterium was observed with the epithermal neutron detector. The ratio of neutron intensity at right angles to the intensity parallel to the x-ray beam was found to be 1.60 ± 0.07 . From this observed ratio and the known variation of photoelectric and photomagnetic cross sections of the deuteron near threshold the value of ϵ_0 for the epithermal neutron detector was calculated to be 130 kev.

Samples of gold and bismuth were irradiated with 10-Mev bremsstrahlung, and the epithermal photoneutrons from these samples do not show any anisotropy outside probable error. Figure 8 shows the photoneutron yield from $\text{Be}(\gamma,n)$ as measured with the epithermal neutron detector as a function of maximum betatron energy.

IV. DISCUSSION

The concept of a statistical model of the nucleus has been developed in great detail by Weisskopf and others. One of the basic premises of the statistical model is that the mode of decay of an excited nucleus is independent of the mode of formation. Another requirement is that the energy-level density of the compound nucleus and the residual nucleus may be expressed by continuous functions. When these requirements are satisfied, one arrives at a photoneutron energy spectrum such as was given in Part II.

A corollary to the statistical model states that the angular distribution of the emitted particles must be isotropic. That is implied in the independence of the mode of formation and the mode of decay of the compound nucleus. Because of the random phase of the many energy states, one would expect that particles emitted from the compound nucleus, not going to the ground state, would be emitted isotropically. In the gamma-neutron reaction any deviation from isotropy would be attributed to the low-lying states of the residual nucleus where the wide spacing of energy levels violates the premise of a statistical model. These concepts of angular distributions of reaction particles in the statistical model are born out in the experiments which are performed. The moderated neutron detector, which detects neutrons up to several Mev equally well,

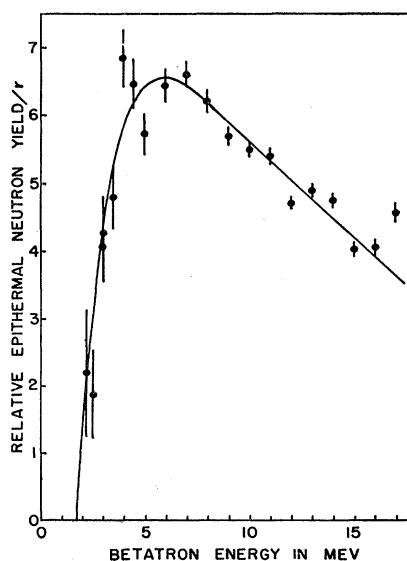


Fig. 8. Relative yield of photoneutrons from beryllium as observed with the epithermal neutron detector.

indicated that the intensity of photoneutrons is very nearly independent of direction. If the angular distributions are expressed in the form $A + B \sin^2\theta$, then the ratio of neutrons contributing to the anisotropic term, $B \sin^2\theta$, to the total number of neutrons is $1.67B/A$. For example, in the case of photoneutrons from bismuth 21 percent of all the neutrons are emitted in a $\sin^2\theta$ distribution (anisotropic), whereas the rest are emitted isotropically. The other elements which were tested with the moderated neutron detector showed smaller anisotropic terms than did bismuth.

Measurements of the angular distributions of photoneutrons with the threshold detectors, $\text{Al}^{27}(n,p)$ and $\text{Si}^{28}(n,p)$, showed a much more pronounced anisotropy than did the moderated neutron detector. The threshold detectors are sensitive to the very energetic neutrons, around 4 Mev, which represent transitions of the compound nucleus to low-lying levels in the residual nucleus. In keeping with the restrictions of the statistical model, it would be the high-energy neutrons which could exhibit a deviation from isotropy if any neutrons did so.

The epithermal neutron detector showed isotropy of photoneutrons from gold and bismuth with energies from zero up to a few kev. The maximum cross section for nuclear absorption of photons is about 6 Mev above the gamma-neutron threshold. Just such a peak has been observed in most gamma-neutron cross sections. This means that most of the epithermal neutrons are emitted from the compound nucleus about 14 Mev above the ground state and the residual nucleus is left in an excited state, 5 or 6 Mev above its ground state. These conditions are ideal for the statistical model; therefore, one would expect the epithermal neutrons to be emitted isotropically with an energy spectrum appropriate to the statistical model.

The concept of a statistical model in the formation and decay of a compound nucleus does not in any way contradict the principles of quantum mechanics. The nucleus and its reaction products must still be considered as a quantum mechanical system. The absorption of the photon to form the compound nucleus and the subsequent emission of a neutron must still conform to the principles of conservation of parity, energy, angular momentum, etc. Under certain conditions however, certain average quantities can be examined,

just as in the kinetic theory of gases the principles of statistical mechanics can be used to derive the general gas laws by considering the average behavior of a large group of molecules. A quantum-mechanical description of the gamma-neutron reaction in a heavy nucleus can disclose several facts about the angular distributions of the particles involved, even when little is known about the specific energy levels.

There is a theorem on the complexity of angular distributions in nuclear reactions which is applicable to the gamma-neutron reaction. It is given implicitly by Myers¹⁸ and shown more explicitly by Eisner and Sachs.¹⁹ Eisner and Sachs state their conclusions as follows: "In a nuclear reaction produced with an unpolarized beam of given orbital angular momentum on an unpolarized target, the angular distribution of the outgoing intensity cannot be more complicated than that of the incoming intensity." To be more explicit, the highest Legendre polynomial necessary to describe the outgoing intensity is $P_{2L}(\cos\theta)$, where L is the orbital angular momentum, in units of \hbar , of the incoming wave. The theorem does not in any way restrict the angular momentum of the outgoing neutron to values equal to, or less than, L , but rather, the limitation on the degree of the highest Legendre polynomial in the intensity arises out of interference between outgoing neutron waves.

Photon absorption usually goes by dipole transition in which case $L=1$. Then the outgoing neutron intensity can be expressed as $a_0 + a_1P_1(\cos\theta) + a_2P_2(\cos\theta)$, where a_0 , a_1 , and a_2 are arbitrary constants. For the purpose of comparison, the observed angular distributions are fitted in the best possible way to the above function. It can be shown that the existence of the second term $a_1P_1(\cos\theta)$ may be attributed to a mixture of dipole and quadrupole absorption of the photon. Strictly speaking, terms up to $P_4(\cos\theta)$ should be included to account for quadrupole effects. However, $P_3(\cos\theta)$ and $P_4(\cos\theta)$ were omitted since some of the data could not be specified uniquely by more than three arbitrary constants.

The author is indebted to D. W. Kerst for his interest and encouragement in this problem.

¹⁸ R. D. Myers, Phys. Rev. **54**, 361 (1938).

¹⁹ E. Eisner and R. G. Sachs, Phys. Rev. **72**, 680 (1947).